


Cite this: *RSC Adv.*, 2024, 14, 9619

Recent advances in DDAH1 inhibitor design and discovery: insights from structure–activity relationships and X-ray crystal structures

Anthony J. Doman,^{ab} Michael V. Perkins,^{id c} Sara Tommasi,^{ab} Arduino A. Mangoni^{abd} and Pramod C. Nair^{id *bdef}

Nitric oxide (NO) is an important signalling molecule which modulates several biological and pathological processes. Dimethylarginine dimethylaminohydrolase 1 (DDAH1) plays a key role indirectly regulating NO concentrations in the body. It has been shown that DDAH1 inhibition may be an effective therapeutic strategy in certain pathological states in which excessive NO is produced. In recent years, specific DDAH1 inhibitors have shown promise in suppressing abnormal neovascularization in cancer. However, the available DDAH1 inhibitors lack potency and selectivity and are mostly arginine-based. Further, these inhibitors display unfavourable pharmacokinetics and have not been tested in humans. Thus, the development of potent, selective, and chemically diverse DDAH1 inhibitors is essential. In this review, we examine the structure activity relationships (SARs) and X-ray crystal structures of known DDAH1 inhibitors. Then, we discuss current challenges in the design and development of novel DDAH1 inhibitors and provide future directions for developing potent and chemically diverse compounds.

Received 1st December 2023

Accepted 15th March 2024

DOI: 10.1039/d3ra08210e

rsc.li/rsc-advances

Introduction

Nitric oxide (NO) is a powerful signalling molecule, crucial for the maintenance of physiological processes and immune defences. The homeostatic regulation of neuronal pathways,¹ vascular tone,² and cytotoxicity in immunity³ depends on tight regulation of NO concentrations. Nitric oxide synthase (NOS) is the enzyme responsible for NO synthesis. Excessive NO production is associated with a wide range of pathophysiological states including multiple sclerosis,⁴ sepsis,⁵ Parkinson's disease,⁶ metabolic dysregulation,⁷ and cancer.⁸ The use of NOS inhibitors may directly inhibit NO production, however, simultaneously blocking its beneficial effects. Therefore, in certain disease states, indirect inhibition of NO synthesis may provide better therapeutic outcomes in regulating excess NO.⁹ Dimethylarginine dimethylaminohydrolase 1 (DDAH1) is a key enzyme involved in the metabolism of asymmetric dimethylarginine (ADMA) to

L-citrulline and dimethylamine.⁹ ADMA and other substrates of DDAH1 (e.g., L-NMMA or monomethyl-L-arginine) function as potent endogenous NOS inhibitors (Fig. 1). NO concentrations are reduced by the accumulation of ADMA and L-NMMA in cells upon inhibition of DDAH1. In recent years, there has been considerable interest in DDAH1 as a potential target for indirect inhibition of NO synthesis in diseases that produce excessive amounts of NO, such as septic shock,¹⁰ and aberrant neovascularization,¹¹ including cancers such as melanoma,¹² prostate cancer,¹³ and breast cancer.¹¹

Two DDAH isoforms (DDAH1 and DDAH2) have been identified in humans, which share ~67% protein sequence homology with distinct tissue distribution.¹⁴ While DDAH1 plays a key role in the NO pathway, it is unclear what role DDAH2 plays. Recently, we demonstrated that DDAH2 does not metabolize ADMA and may have an ADMA independent function.¹⁵ Given previously known DDAH inhibitors were based on inhibiting ADMA conversion to citrulline, it is likely these compounds inhibit DDAH1 only.

Novel inhibitors targeting DDAH1 have been developed as a result of the crucial importance of fine regulation of the NO pathway (Table 1). For instance, human DDAH1 inhibitor **ZST316** (**20**) was shown to attenuate vasculogenic mimicry and cell migration in triple negative breast cancer (TNBC) cells.¹¹ Also, DDAH1 inhibitor **DD1E5** inhibits the proliferation of human prostate cancer (PCa) cells and NO production while decreasing the amount of vascular endothelial growth factor (VEGF), thereby inhibiting angiogenesis and tumor progression in mice.¹³

In this study, we review the literature of known inhibitors of hDDAH1 over the past two decades (patents not included)

^aDepartment of Clinical Pharmacology, Flinders Medical Centre, Southern Adelaide Local Health Network, Adelaide, Australia

^bDiscipline of Clinical Pharmacology, College of Medicine and Public Health, Flinders Medical Centre, Flinders University, Adelaide, Australia. E-mail: pramod.nair@flinders.edu.au; Tel: +61-8-82043155

^cCollege of Science and Engineering, Flinders University, Adelaide, Australia

^dFlinders Health and Medical Research Institute, Flinders University, Adelaide, Australia

^eCancer Program, South Australian Health and Medical Research Institute (SAHMRI), University of Adelaide, Adelaide, SA, Australia

^fDiscipline of Medicine, Adelaide Medical School, The University of Adelaide, Adelaide, SA, Australia



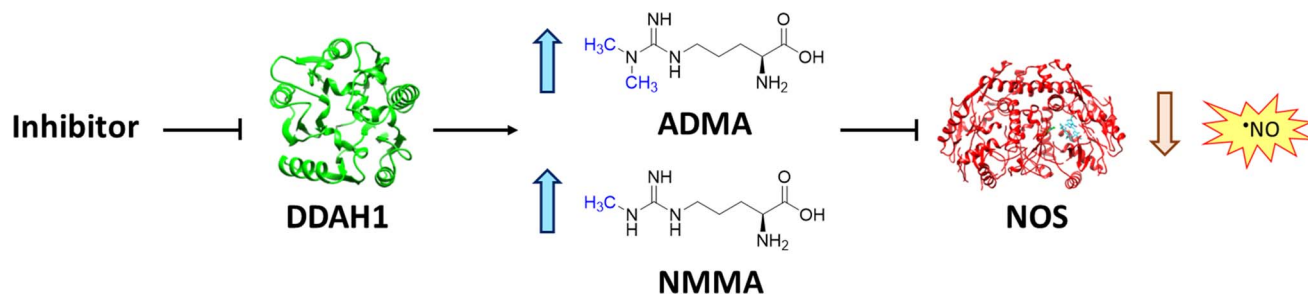


Fig. 1 DDAH1 substrates and NOS inhibitors ADMA and NMMA.

Table 1 Evolution of the major DDAH1 inhibitors

| Name | Chemical structure | Activity | Author | Year of publication | Reference |
|----------------------|--------------------|--|--------------------------|---------------------|-----------|
| 4124W (1) | | $IC_{50} = 1510 \mu M$ | MacAllister | 1996 | 16 |
| L-257 (13) | | $K_i = 13 \mu M$ | Rossiter <i>et al.</i> | 2005 | 18 |
| L-VNIO (25) | | $K_i = 2 \mu M$; $IC_{50} = 13 \mu M$ | Kotthaus <i>et al.</i> | 2008 | 26 |
| 4-HNE | | $IC_{50} = 50 \mu M$ | Forbes <i>et al.</i> | 2008 | 46 |
| L-IPO (59) | | $K_i = 52 \mu M$ | Wang <i>et al.</i> | 2009 | 32 |
| 14 ^a (60) | | $K_i = 7.5 \mu M$ | Wang <i>et al.</i> | 2009 | 32 |
| Ebselen | | $IC_{50} = 0.33 \mu M$ | Linsky <i>et al.</i> | 2011 | 47 |
| Lansoprazole | | $IC_{50} = 51 \mu M$ | Ghebremariam | 2013 | 48 |
| PD404182 | | $IC_{50} = 9 \mu M$ | Ghebremariam | 2014 | 49 |
| ZST316 (20) | | $K_i = 1 \mu M$; $IC_{50} = 3 \mu M$ | Tommasi <i>et al.</i> | 2015 | 22 |
| DD1E5 | | $K_i = 2 \mu M$ | Kami Reddy <i>et al.</i> | 2019 | 13 |
| 8a ^a (46) | | $K_i = 18 \mu M$ | Lunk <i>et al.</i> | 2020 | 28 |

^a Published identification number.



considering their structure activity relationships (SARs) and X-ray crystal structures. Furthermore, we discuss current challenges in designing and developing novel inhibitors for DDAH1 and suggest future directions.

Butanoic acids as DDAH1 inhibitors

In one of the earliest studies, MacAllister *et al.*¹⁶ identified **1** (**4124W**) as a weak inhibitor of rat and human DDAH ($IC_{50} = 416, 250 \mu M$) respectively. This inhibitor is a short-chained analogue of L-NMMA and the first known reversible inhibitor of mammalian DDAH. This compound exhibited endothelium-dependent vasoconstriction in mouse models (evidence of indirectly inhibiting NO production),¹⁷ and was chosen as the lead compound for reversible DDAH inhibitor design by Rossiter *et al.*¹⁸

Optimisation of **1** was initiated by modifying the N^{ω} guanidine atom, Fig. 2. The short carbon chain length of **1** was initially maintained by changing the substituents at the guanidine N^{ω} atom. Under these conditions, **1** did not show promising activity (**1**, $IC_{50} = 1510 \mu M$). Increasing the C chain from methyl (**1**) to ethyl (**2**) further improved activity (**2**, $IC_{50} = 300 \mu M$). Greater improvement was observed introducing an O atom, forming 2-methoxyethyl (**3**, $IC_{50} = 189 \mu M$). However, activity decreased when introducing isopropoxyethyl functional group (**4**, $IC_{50} = 301 \mu M$). Dual methyl groups at this position gave similar potency (**5**, $IC_{50} = 325 \mu M$) but also inhibited eNOS and was abandoned. Interestingly, introducing a sterically larger piperidinyl group marginally improved activity (**6**, $IC_{50} = 264 \mu M$). The most potent analog, 2-methoxyethyl, was retained

for further studies (**3**, $IC_{50} = 189 \mu M$). Ester modifications at the carboxyl end of **3** were further optimised.

The short methyl ester modification further improved ligand activity (**7**, $IC_{50} = 96 \mu M$) compared to **3** ($IC_{50} = 189 \mu M$). Linear ethyl ester modification moderately improved ligand activity (**8**, $IC_{50} = 159 \mu M$). Extension of the aliphatic C chain to propyl ester (**9**, $IC_{50} = 111 \mu M$) and butyl ester (**10**, $IC_{50} = 113 \mu M$) improved DDAH inhibition. Interestingly, a larger aliphatic benzyl group gave the efficient ligand activity (**11**, $IC_{50} = 27 \mu M$) but was abandoned by the authors due to poor solubility. Isopropyl ester (**12**, $IC_{50} = 189 \mu M$) did not alter ligand activity compared to the standard carboxy acid group (**3**, $IC_{50} = 189 \mu M$). As a result, developing a methyl substitution (**7**) was one of the obvious choices for the authors.

Arginine derivatives as DDAH1 inhibitors

Despite possible NOS inhibition, Rossiter *et al.*¹⁸ explored arginine derivatives (L-arginine is a substrate of NOS) for developing DDAH1 inhibitors.^{19,20} Compound **7** was further developed to arginine derivatives by extending the carbon backbone which improved DDAH1 activity significantly. Carboxylic acid motif **13** ($IC_{50} = 22 \mu M$, Fig. 2) gave similar potency to the methyl ester (**14**, $IC_{50} = 20 \mu M$) and was favoured, as **14** is anticipated to be converted to **13** by liver carboxylesterases.²¹ Additionally, the removal of carboxy or 2-amino groups, R-enantiomers of the most active compounds, and cyclic analogues did not improve DDAH1 inhibition. Overall, **13** was identified as a potent and selective DDAH1 inhibitor. The methyl ester analogue **14** exhibited elevated plasma ADMA concentrations indicating DDAH1 inhibition in mouse models.

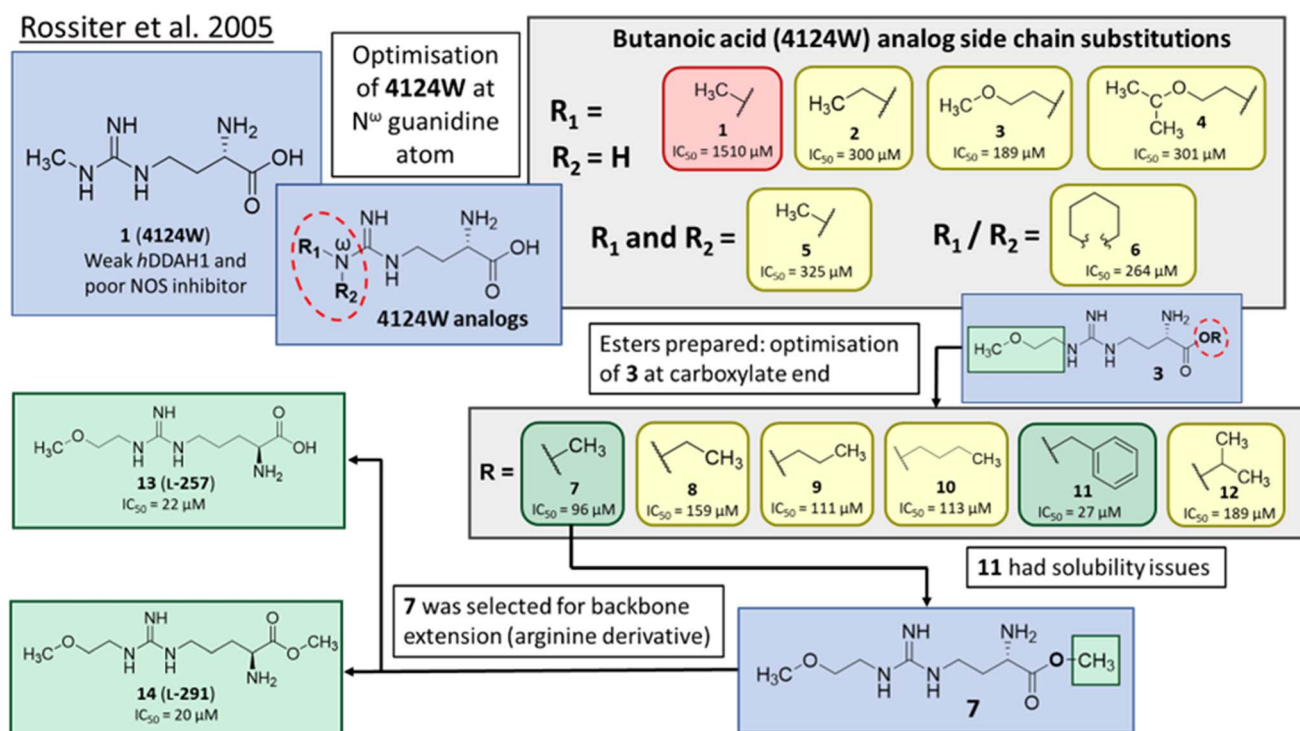


Fig. 2 Development of DDAH1 inhibitor L-257 (**13**)¹⁸ from 4124W (**1**).¹⁶ Optimisation at N^{ω} -guanidine and carboxylate ends. N^{ω} side chain and carboxy substitutions shown in green ($K_i < 100 \mu M$); yellow ($K_i = 100-1000 \mu M$) and red ($K_i > 1000 \mu M$).

Tommasi et al. 2015

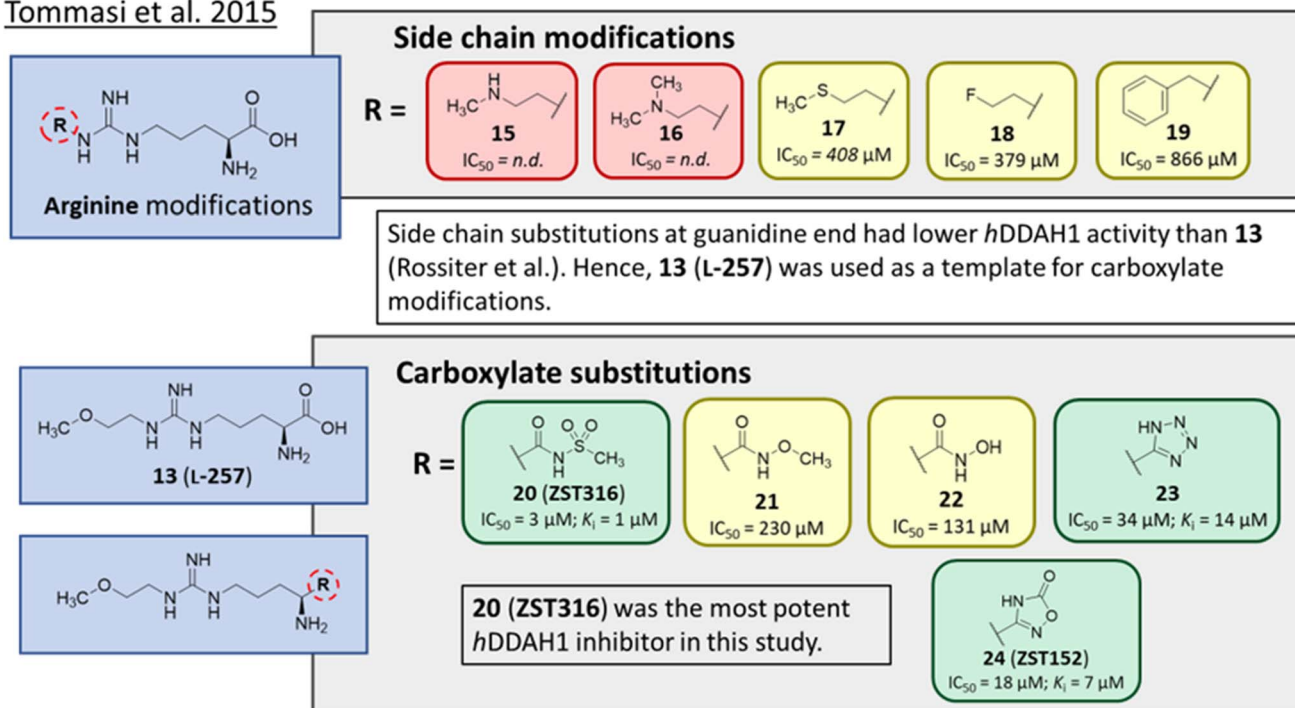


Fig. 3 Development of *h*DDAH1 inhibitor ZST316 (**20**)²² from L-257 (**13**).¹⁸ R group substitutions shown in green (K_i and $IC_{50} < 100 \mu M$); yellow ($IC_{50} = 100\text{--}1000 \mu M$) and red ($IC_{50} = n.d.$). n.d. = not determined when inhibition $< 50\%$ at 1 mM.

Arginine side chain and carboxylate bioisosteres of L-257

Tommasi *et al.*²² developed a set of inhibitors based on **13**, due to the selectivity of this scaffold for DDAH over NOS and arginase.^{18,23} Two classes of inhibitors were explored: **13** side chain derivatives (substitution at the 2-methoxyethyl end) and **13** carboxylate bioisosteres, Fig. 3. 1,2,3-Triazoles with different chemical structures to **13** were also explored, however, these compounds displayed poor solubility and DDAH1 inhibition.

Side chain derivatives with diverse substituents were investigated with alterations at the 2-methoxyethyl end of **13**. Replacement of an oxygen for a nitrogen at the 2-methoxyethyl end gave **15** ($IC_{50} = n.d.$; 29% at 1 mM) with weaker affinity for *h*DDAH1. A modified tertiary amine group (**16**, $IC_{50} = n.d.$; 14% at 1 mM) also gave poor inhibition. Hydrophobic interactions were explored using methylthio group (**17**, $IC_{50} = 408 \mu M$), with moderate *h*DDAH1 inhibition. Altered electronegativity using 2-fluoroethyl group (**18**, $IC_{50} = 379 \mu M$) was the best of this series but still less potent than **13** ($IC_{50} = 22 \mu M$, Fig. 2). A benzyl group side chain was investigated, but did not significantly inhibit *h*DDAH1 (**19**, $IC_{50} = 866 \mu M$).

All carboxylate bioisosteres inhibited the enzyme at 1 mM concentrations (79–98%). The most potent of this series was acylsulfonamide (**20**, **ZST316**, $IC_{50} = 3 \mu M$; $K_i = 1 \mu M$). There was a decrease in inhibition of *h*DDAH1 when the acidity of the bioisosteric replacement was less than the carboxylate group of **13**, O-methylhydroxamic group (**21**, $IC_{50} = 230 \mu M$) and the hydroxamic group (**22**, $IC_{50} = 131 \mu M$). However, introducing bioisosteres with multiple heteroatoms, such as tetrazole (**23**,

$IC_{50} = 34 \mu M$; $K_i = 14 \mu M$) and oxadiazolone (**24**, **ZST152**, $IC_{50} = 18 \mu M$; $K_i = 7 \mu M$) significantly restored *h*DDAH1 inhibition. According to the authors, positively charged residues at the *h*DDAH1 active site may facilitate the binding of inhibitors with greater acidity near the carboxylate end of the (**13**, L-257) scaffold.

Molecular dynamics (MD) simulations of **20** revealed a novel binding mode within the *h*DDAH1 binding site, Fig. 4. It was shown that this inhibitor induces a change in the rotamer position of Arg145 (protein numbering Met = 1) by exploiting a new binding pocket. Aided by main-chain atoms from helix 4 residues, a sulfonyl O atom forms four H-bonds with the main

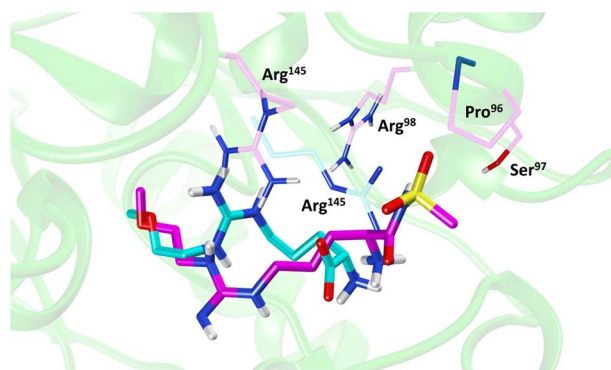


Fig. 4 Binding mode of ZST316 from molecular dynamics simulation²² overlaid on the X-ray crystal structure of L-257 bound to *h*DDAH1 (pdb 2jaj). Image created using UCSF Chimera.



chain NH of Pro96 and Ser97, with the side chain OH of Ser97 and with the side chain NH of Arg98. The second O atom of the sulfonyl group H-bonds with the side chain NH of Arg145. The authors proposed that these novel interactions of **20** (not noted in **13**) within DDAH1 are likely responsible for increased DDAH1 inhibition.

Ornithine and arginine derivatives as DDAH1 inhibitors

Ornithine derivatives with an amidine functional group (**L-VNIO** and associated analogs) were previously identified as potent NOS inhibitors.^{24,25} Amidines are bioisosteres of guanidine and expected to have similar *h*DDAH1 potency as derivatives of *L*-arginine. Kotthaus *et al.*²⁶ integrated similar analogs by substituting amidine side chains, evaluating linear aliphatic and alkenyl side chain groups. These derivatives probed the effect of chain length and double bonds on *h*DDAH1 inhibition, Fig. 5.

Ornithine derivatives with an amidine substructure and simple aliphatic substitutions were evaluated for DDAH1 inhibition. Ethylene was found to be the most potent from this series (**25**, **L-VNIO**, $K_i = 2 \mu\text{M}$). Removing the electron density and changing the geometry of the terminal C atom from a planar sp^2 hybridised π -bond (**25**) to a tetrahedral sp^3 hybridised ethyl group (**26**, $K_i = 32 \mu\text{M}$) did not show significant improvement in DDAH1 inhibition. Also, extending the C chain to form the *trans*-alkenyl analog (**27**, $K_i = 36 \mu\text{M}$) did not improve inhibitory activity. Smaller substitutions such as methyl (**28**, $K_i = 145 \mu\text{M}$) and hydrogen (**29**, $K_i = \text{n.d.}$) gave unfavourable *h*DDAH1 inhibition.

Arginine derivatives with a guanidine substructure (**30–37**, Fig. 5) were developed to improve *h*DDAH1 inhibition. These molecules were compared to **13** ($K_i = 13 \mu\text{M}$, Fig. 5) as they all contain guanidine and were expected to bind similarly to the DDAH1 active site. Removing the O atom from 2-methoxyethyl end decreased ligand activity (**30**, $K_i = 90 \mu\text{M}$). However, π -electron density at the terminal position (**31**, $K_i = 58 \mu\text{M}$) partly restored ligand activity. Extending the C chain of **31** by 1C atom did not improve DDAH1 inhibitory effects (**32**, $K_i = 57 \mu\text{M}$). Further enhancement was observed by the alkyne derivative (**33**, $K_i = 17 \mu\text{M}$), suggesting stronger electronic effects (sp hybridisation) at this position favouring *h*DDAH1 inhibition. The least active compounds in the guanidine series had side chain substitutions with electron withdrawing properties, *e.g.*, trifluoromethyl (**34**, $K_i = \text{n.d.}$) and nitro (**35**, $K_i = \text{n.d.}$) groups. Analogs with slightly larger steric bulk, such as N^ω -(2-carbamoyl-ethyl)-*L*-arginine (**36**, $K_i = \text{n.d.}$) and the cyclic N^ω -morpholinyl-*L*-arginine (**37**, $K_i = \text{n.d.}$) were also less effective than the alkenyl derivatives. Importantly, the electron donating 2-methoxyethyl group (**13**, $K_i = 13 \mu\text{M}$) was more active than the electron withdrawing groups (**34** and **35**, $K_i = \text{n.d.}$) or those that are sterically larger (**36** and **37**, $K_i = \text{n.d.}$). Additionally, it appears the *h*DDAH1 active site is sensitive to the size of functional groups at the N^ω atom position, as relatively sterically large substitutions at this position appear to hinder *h*DDAH1 inhibition. Additionally, the rigidity of the functional group at the N^ω position is undesirable as shown in ref. 37. As a result, flexibility of substitution may be a prerequisite for optimal binding.

Kotthaus et al 2008

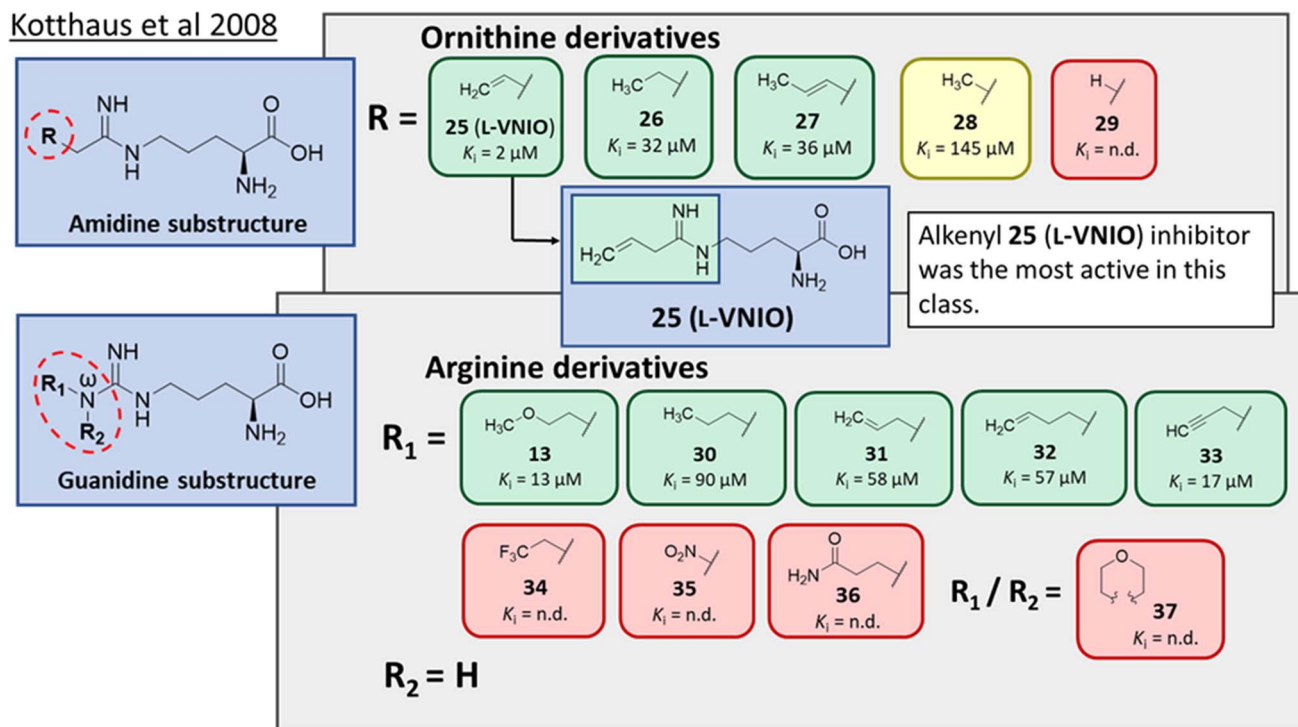


Fig. 5 Development of *h*DDAH1 inhibitors using amidine and guanidine substructures.²⁶ *L*-257 (**13**) activity as K_i value. R group substitutions shown in green ($K_i < 100 \mu\text{M}$); yellow ($K_i = 100\text{--}1000 \mu\text{M}$) and red ($K_i = \text{n.d.}$). n.d. = not determined when inhibition $< 50\%$ at 1 mM.

Testing of the ornithine and arginine derivatives against NOS showed potent inhibition towards all NOS isoforms (25–29 were previously known inhibitors of NOS). However, 13, 27, 32, 34, 36 and 37 were less effective NOS inhibitors. The inhibition of *h*DDAH1 by 27 and 32 was particularly interesting since there was selectivity for *h*DDAH1 over NOS.

The authors suggested that elongation of the alkenyl side chain may improve selectivity towards DDAH1 over NOS. This hypothesis is supported by the work of Rossiter *et al.*,¹⁸ who demonstrated that larger substitutions such as 2-isopropoxyethyl (4, IC_{50} = 301 μ M, Fig. 2) may bind to the DDAH active site. This is further supported by the fact that molecules larger than $N^{(w)}$ propyl cannot fit inside the active site of NOS,²⁷ where N^5 -(1-iminoethyl)-L-ornithine (Butyl-L-NIO) inhibits NOS weakly (>1.5 mM).²⁵

The first *h*DDAH1 inhibitor with amidine substructure having excellent DDAH1 activity was 25 (L-VNIO, K_i = 2 μ M, Fig. 5). However, this compound was not selective over NOS when compared to 13 (L-257, K_i = 13 μ M, Fig. 5).

Advancement of ornithine and arginine DDAH1 inhibitors

Rossiter *et al.*¹⁸ previously developed 13 (L-257, Fig. 2 and 5), a selective inhibitor towards *h*DDAH1 over NOS and arginase. Likewise, Kotthaus *et al.*²⁶ aimed to develop more potent and selective *h*DDAH1 inhibitors using ornithine and arginine side-chain substitutions, Fig. 5. They identified 25 (L-VNIO, K_i = 2 μ M) that was found to be more potent than 13 (K_i = 13 μ M) but less selective towards *h*DDAH1 over NOS and arginase,²³ prompting further investigation. Furthermore, it was proposed that the 2-methoxyethyl substituent of 13 is not favourable for binding to the NOS active site (possibly a consequence of inappropriate steric and/or electrostatic interactions) hence more selective for DDAH1.^{23,26} Therefore, following from Kotthaus study, Lunk *et al.*²⁸ investigated a diverse range of methoxy and alkenyl substitutions by shortening and extending the C side chain, leading to improved potency and selectivity towards *h*DDAH1. Major advancements from this study include the identification of a novel selective *h*DDAH1 inhibitor with a novel binding mode. In addition, it provided conclusive evidence that the α -carboxy group is dispensable for potent *h*DDAH1 inhibition for arginine-based inhibitors.

Ornithine and arginine derivatives having amidine and guanidine substructures respectively are shown in Fig. 6. Ornithine analogs with a 2-methoxy substituted side chain (38 and 39) was most potent when both carboxy and amine groups were present (38, K_i = 73 μ M) and less potent when removing the carboxy but retaining the amine group (39, K_i = 983 μ M). Similarly, analogs with a 3-methoxy side chain (40 and 41) were more potent with the carboxy group (40, K_i = 9 μ M) than without (41, K_i = 1446 μ M). Although 40 gave similar potency to 13 (K_i = 13 μ M, Fig. 5), was less selective over NOS and arginase. Increasing the side chain length to 4-methoxy restored *h*DDAH1 inhibition somewhat (42, K_i = 156 μ M) but activity was again lost without the carboxy group (43, K_i = n.d.). Interestingly, poor ligand activity was observed when shortening the main C chain (44, K_i = n.d., supported by previous results of *nor*-arginine and *nor*-ornithine butanoic acid analogs¹⁸) or when a propene side

chain was introduced (45, K_i = 768 μ M). In summary, ornithine analogs without the α -carboxy group were less potent than those with both the α -carboxy and amine groups.

Arginine derivatives incorporating guanidine were compared to 13 (K_i = 13 μ M, Fig. 5).²⁶ Interestingly, the most potent analog from this series incorporated the 2-methoxyethyl side chain with the removal of the α -carboxy group (46, K_i = 18 μ M) which gave comparable potency and selectivity to 13 over NOS and arginase. Conversely, absence of the α -amine group but presence of the α -carboxy group decreased inhibitory potency (47, K_i = 489 μ M). Pentyl substitution (48, K_i = 2815 μ M) or isopentyl (49, K_i = 2763 μ M) was not favourable towards *h*DDAH1 inhibition. However, butyl amine (50, K_i = 59 μ M) and amino pentanoic acid (51, K_i = 57 μ M) groups restored ligand activity.²⁸

Notably, arginine analog 46 (K_i = 18 μ M) gave comparable potency and selectivity to L-257 (13, K_i = 13 μ M, Fig. 5) over NOS and arginase. This suggests the electronic effects of 2-methoxyethyl guanidine group contributes significantly to *h*DDAH1 binding. Importantly, the equivalent amidine analog (41, K_i = 1446 μ M) was not as effective, indicating that the positive charge induced by electron delocalisation of the guanidine group is essential for *h*DDAH1 inhibition. Interestingly, the decarboxylated guanidines (46 and 50) were more selective towards *h*DDAH1 over NOS and arginase than their carboxylate partners. This suggests the α -carboxy group is dispensable for potent and selective *h*DDAH1 inhibition using arginine (guanidine) derivatives. Overall, removal of the α -carboxy group was tolerated by guanidine (arginine) but not amidine (ornithine) functional groups.

Binding modes of 13 (pdb 2jaj) and inhibitor 46 (pdb 6szp) bound *h*DDAH1 were defined using X-ray crystallography. Superposition of 13 and 46 show almost identical binding modes, Fig. 7. Comparison of these inhibitors bound to *h*DDAH1 (ref. 28) all show the α -amino group positioned tightly by H-bonds, interacting with the side chain of Asp73 and backbone carbonyl interactions of Leu30 and Val268. This highlights the importance of the α -amine group likely due to the optimal geometry of all H-bond partners. Noticing the similar alignment of the butyl chains of 13 and 46, orientation appears to originate from their guanidine groups. Crystal structures of 13 and 46 show the outward pointing guanidine NH interacts with Asp79 and the aminobutyl substituted guanidino-NH with Asp79. A second set of interactions bind the methoxyethyl-substituted distal guanidino-NH on the opposite side in place *via* side chain and backbone carbonyl oxygens of Asp269. Therefore, Asp79 and Asp269 residues form 2 clamps securing the guanidine group in place. These clamps influence the positioning of the 2-methoxyethyl and 4-aminobutyl groups in the active site. This strong interaction of guanidine and the two Asp guanidine clamps induce a rotation of His173 out of its apo (native) position, causing an outward twist of Arg145. This is opposite to the N^5 -(1-iminopentyl)-L-ornithine (L-IpEO)²⁹ and L-citrulline³⁰ binding modes (pdb 3p8p and 2jai respectively), as the respective amidino or urea groups cannot interact with Asp79/269 in the same way. The difference is the greater flexibility of the pentyl (L-IpEO) chain and the amino acid side chain (L-IpEO, L-citrulline), compared with 13 and 46. The authors suggest the higher basicity of guanidine also induces stronger binding compared to amidine or urea. Lacking the guanidine



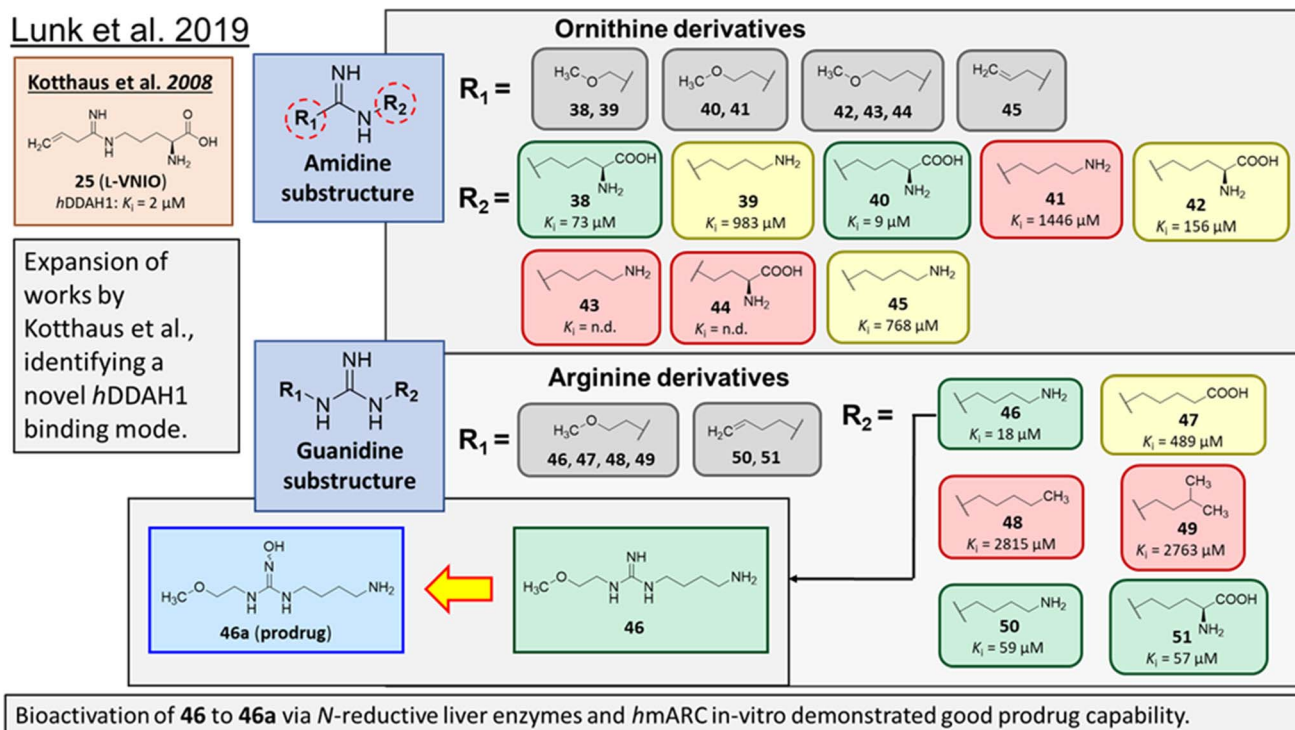


Fig. 6 Development of *hDDAH1* inhibitor 46 from guanidine substructure.²⁸ R group amidine and guanidine substitutions are shown in green ($K_i < 100 \mu\text{M}$); yellow ($K_i = 100\text{--}1000 \mu\text{M}$) and red ($K_i > 1000 \mu\text{M}$ or n.d.). n.d. = not determined when inhibition $< 20\%$ at 1 mM.

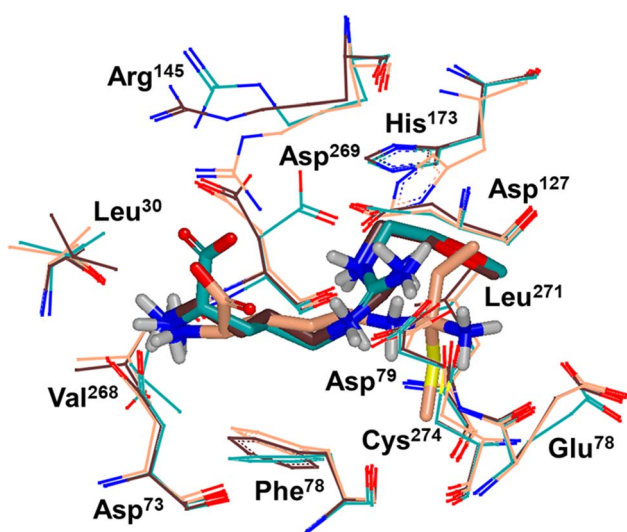


Fig. 7 X-ray crystal structure overlay of *hDDAH1* bound to 13 (L-257) (cyan, pdb 2jaj), 46 (brown, pdb 6szp) and 59 (L-IPO) (tan, pdb 3i4a). H, N, O and S atoms are shown in white, blue, red and yellow respectively. Residues numbered, Met = 1. Image created using OpenEye VIDA.

preorientation interactions of an ornithine (amidine) based inhibitor, appears to have a higher degree of freedom enabling interaction of the α -carboxy group with Arg145. This interaction is responsible for potent binding and without the COOH group, results in loss of activity towards *hDDAH1*. Interestingly, the gauche conformation of the butyl chain (46) is tolerated due to

strong binding *via* the guanidino and α -amino groups. In contrast, amidine groups adopted anti conformations suggesting weaker interactions. (This guanidine binding of the butyl chain appears to make the Arg145 interaction dispensable, but the α -amine group is necessary for potent binding).

Drug-like qualities of 46 were considered for optimal absorption *via* passive diffusion. As 13 has zwitterionic character, absorption was expected to be mediated by active uptake of amino acid transporters. However, this is feasible for the primary amine of 46, but its guanidine component would be fully charged under physiological conditions preventing membrane transport by passive diffusion. Therefore, a prodrug *N*-hydroxyguanidine 46a, formed by hydroxylating the central N^ω atom of guanidine of 46 was further investigated.

As demonstrated in their previous works, *N*-hydroxylated guanidines are effectively bioactivated by the mARC (mitochondrial amidoxime-reducing component) containing N-reductive enzyme system *in vitro*, with evidence of bioactivation using this system *in vivo*.³¹ Therefore, 46a is expected to be reduced to 46 efficiently in the liver *via in vivo* bioactivation.

Investigations of distinct subcellular liver fractions showed highest reduction rates of 46a in outer mitochondrial membrane vesicles (OMV) followed by mitochondria and liver homogenate. Additionally, incubations with reconstituted heterologously expressed human mARC-1 and mARC-2 isoenzymes confirmed that 46a is a particularly good substrate of the N-reductive enzyme system. Based on these results, there is high probability of acceptable bioavailability of 46a. One concern was the chemical stability of *N*-hydroxyguanidines,

however, **46a** was stable at different pH's over 24 h at 37 °C. Both the guanidine and prodrug **46a** showed excellent profile with respect to cell toxicity/viability that will be useful as a pharmacological toolset.

Irreversible DDAH1 inhibitors

Wang *et al.*³² developed dual NOS/DDAH1 inhibitors from ornithine derivatives, expected to affect NO biosynthesis greater than single targeted compounds. A set of previously known NOS inhibitors were selected for study, (**52–57**, Fig. 8). *S*-Alkyl isothioureas (**52–54**) and aminoguanidines (**55** and **56**) were initially assayed but were not respective substrates or inhibitors of *h*DDAH1 so were not pursued further by the authors. Benzyl amidine based **1400W** (**57**) (selective iNOS inhibitor) did not inhibit *h*DDAH1 at concentrations <1 mM. However, alkyl amidine inhibited weakly (**58**, **L-NIO**, $K_i = 990 \mu\text{M}$), showing potential for dual NOS/DDAH1 inhibitors. Wang *et al.*³² proposed the α -amino and carboxylate groups may contribute to binding in the active sites of NOS and DDAH1, which was validated by Lunk *et al.*²⁸ Alternatively, an expanded set of alkyl-substituted ornithine derivatives were synthesised and assayed towards DDAH1 and compared to NOS inhibition.

Extending the carbon chain of **L-NIO** (**58**, $K_i = 990 \mu\text{M}$) by 1 methyl group to N^5 -(1-iminopropyl)-L-ornithine (**L-IPO**, **59**, $K_i = 52 \mu\text{M}$, Fig. 8) increased *h*DDAH1 potency by 20-fold. Extending **59** by an additional 2 methyl groups (**60**, $K_i = 7.5 \mu\text{M}$) increased potency a further 7-fold. Branching the alkyl chain did not improve potency. The extension of the carbon chain decreased *h*DDAH1 ligand activity (**61**, $K_i = 110 \mu\text{M}$) suggesting space at the active site is limited, however, selectivity over NOS is increased. The trend of

side chain substitutions is similar for both *h*DDAH1 and *h*NOS. For example, as the number of carbon atoms is increased, the affinity towards each enzyme decreases albeit with different magnitudes.

X-ray crystal structure³² shows continuous electron density between the active site Cys274 and the amidino carbon (C^5) of **59** (Fig. 7), indicating covalent bond formation suggesting a tetrahedral sp^3 complex. Notably, solution studies suggest this compound exhibits a reversible covalent competitive inhibition. The orientation of the (R)-inhibitor complex directs the orientation of the terminal side chain methyl group in the same pocket as the substrate's leaving group (**ADMA**, $N^w\text{-CH}_3$). This may indicate hydrophobic interactions with Leu271. The amidine N^w atom also appears to make a H-bond or ionic interaction with the carboxylate side chain O atom of Glu78. Both charged and hydrophobic interactions of the amidine group contribute to the affinity of **59** towards *h*DDAH1. This was demonstrated using site-directed mutagenesis studies of amino acid residues within the DDAH1 binding site.

A follow-up study by Lluís *et al.*,²⁹ showed that compound **60** ($K_i = 7.5 \mu\text{M}$, Fig. 8) showed a similar binding mode to **59** ($K_i = 52 \mu\text{M}$). The X-ray crystal structure showed a covalent bond between Cys274 and C^5 atom of **60** with tetrahedral geometry. Additionally, the carboxylate and amino groups of the ligand make non-covalent interactions with the side chain carboxylate of Asp73 and carbonyl O atoms of Leu30/Val268. The N^e/N^w amidine atoms (either side of C^5) of **60** form H-bonds with side chain O atoms of Asp79. The alkyl substituent of **60** additionally forms hydrophobic contacts in the active site pocket made up of Leu271, His173 and Gly129. The alkyl substituent of **60** is also packed against His173 more orderly than **59**, likely adding additional van

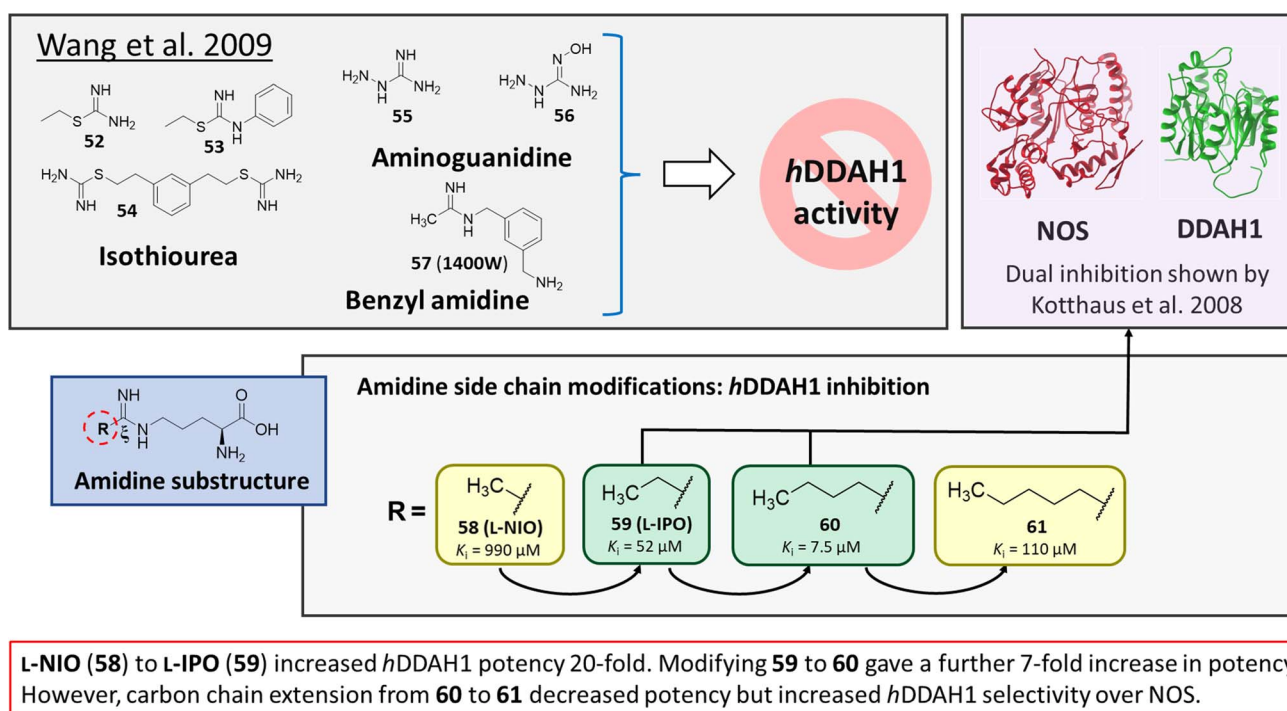


Fig. 8 Rational drug design by Wang *et al.*³² R group substitutions shown in green ($K_i < 100 \mu\text{M}$) and yellow ($K_i = 100\text{--}1000 \mu\text{M}$).

der Waals forces increasing potency. Overall, Wang *et al.*³² found that NOS inhibition requires amidines with alkyl substituents between 2 and 5 carbons in length (**58**, **59**, **60**) but DDAH1 inhibition requires between 3 and 6 carbons in length (**59**, **60**, **61**).

Structure based design and discovery of DDAH1 inhibitors

X-ray crystal structures of bacterial (*Pseudomonas aeruginosa*)³⁰ and mammalian (bovine³³ and human³⁴) DDAH1 have been resolved. The DDAH1 enzyme is similar to the arginine/glycine amidino transferases,³⁰ consisting of a 5 stranded α/β propeller-like fold where the substrate binds in the centre of a “barrel” or cavity at the protein centre and undergoes catalysis (Fig. 9). The barrel at one end is closed by a lid or “flap” made from a looped polypeptide chain. The DDAH1 active site lies in a negatively charged cleft at the centre of the barrel of its propeller-like fold.

The first human X-ray crystal structures of DDAH1 were resolved in the presence of **13** (pdb 2jaj) and citrulline (pdb 2jai),³⁴ where residues Cys274, His173 and Asp127 (protein numbering Met = 1) form the catalytic triad (associated with substrate metabolism). Key H-bonding interactions were shown between guanidine atoms (N^{ω} and N^{δ}) and Asp79.³⁴ The aliphatic portion of the ligand (**13**) backbone packs against Phe76. The amino N atoms form H-bonds with Asp73 and to the main chain O atoms of Leu30 (part of the “lid” region) and Val268. Notably, different orientations of His173 and Arg145 side chains were observed when *h*DDAH1 is bound to L-citrulline (pdb 2jai),³⁴ suggesting ligand induced conformational differences in the DDAH1 binding site.

A comparison of an irreversible covalent inhibitor (**59**, pdb 3i4a, Wang *et al.*³²) to two reversible inhibitors, **13** and **46**, revealed similarities and differences in binding mode and amino acid side chain flexibility, (Fig. 7). The backbone of **13** and **46** has a similar mode of ligand binding, whereas **59** has a distinctly different position. When compared with both reversible inhibitors (**13** and **46**), His173 and Leu30 align differently with **59** at the DDAH1 binding site. It is not surprising that Cys274 adopts a different orientation when covalently bound to **59** than the reversible inhibitors. However,

residues from **59** (Asp73 and Glu78) show similar conformations as those of **46** bound *h*DDAH1, suggesting removal of the carboxy group may activate the binding site similarly to **59**. Alternatively, when **13** is bound to *h*DDAH1, Leu30, Asp73 and Glu78 are positioned slightly differently than **46** and **59**.

Only two studies have reported the utilisation of X-ray crystal structures in the discovery of diverse and novel DDAH1 inhibitors.^{35,36} However, none of these studies have optimised the identified compounds (non-arginine scaffolds) into potent DDAH1 inhibitors. Hartzoulakis *et al.*³⁶ identified potent *Pa*DDAH1 inhibitors with different chemical structures than typical arginine-based inhibitors. A database of 308 000 commercially available compounds were filtered to remove non-drug-like compounds, reducing the number to ~260 k. Reciprocal nearest neighbour (RNN) packing algorithm was then used to generate a second subset of active compounds, reducing the total number to 35 000 structures. Fragment based docking was conducted using FlexX. The top 200 ranked molecules were assessed for binding at the *Pa*DDAH active site (at least 1 H-bond between protein and ligand). Out of the top scored compounds, 90 were purchased and screened using colorimetric assay. Two potent actives (**62**, **63**) were identified from this study (Fig. 10). However, the most potent inhibitor **62** from this study did not inhibit *h*DDAH and several compounds showed poor solubility.^{26,36} Thus, this study highlights that *Pa*DDAH1 may not be an optimal screening system for developing human DDAH1 inhibitors due to differences in the ligand binding site.

In another study, Linsky *et al.*³⁵ performed a high through-put screening (HTS) of 4000 molecules against *Pa*DDAH and *h*DDAH1 isoforms to find a DDAH inhibitor with diverse structure. This HTS utilised an alternative DDAH substrate, *S*-methyl-L-thiocitrulline, to produce an alternative product, methanethiol. This

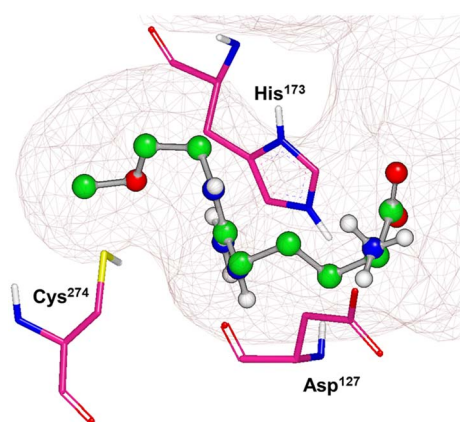


Fig. 9 X-ray crystal structure of *h*DDAH1 (pdb 2jaj), with key catalytic residues displayed. Image created using OpenEye VIDA.

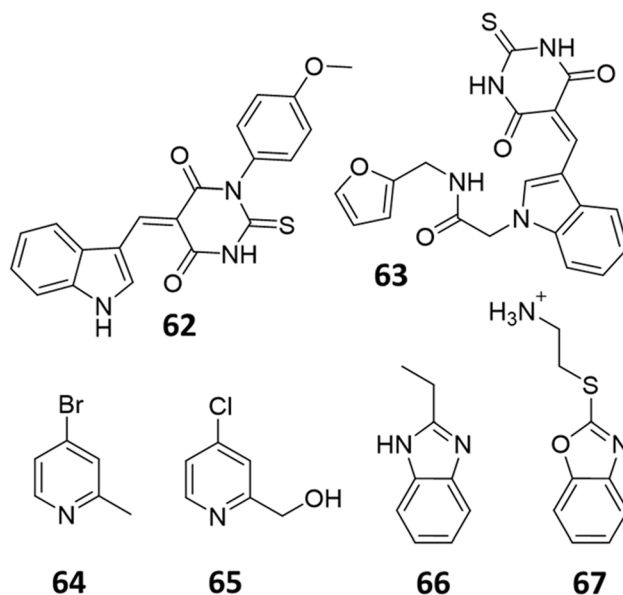


Fig. 10 *Pa*DDAH1 inhibitors **62** and **63**, identified by Hartzoulakis *et al.*³⁶ via virtual screening and hit analysis. *h*DDAH1 inhibitors **64**, **65**, **66** and **67**, identified by Linsky *et al.*³⁵ via fragment based high-throughput screening (HTS).

thiol is detected by chromogenic or fluorogenic reagent and this increase in signal is compared against control wells to observe any inhibition by library compounds. Both isoforms (*PaDDAH* and *hDDAH*) were assayed with the intention of increasing the probability of finding DDAH inhibitors. From a 4000-member fragment library, 101 unique molecules were identified with potential inhibition for *PaDDAH* and *hDDAH1*. These “hits” were manually categorized by structure and a representative from each was repurchased for validation tests, resulting in a total of 107 compounds that progressed to further study. A series of validation tests were designed to eliminate false positives, where 68% of the initial primary hits were identified as false positives due to assay interference. Two additional validation tests were used to eliminate false positives to the 31 hits identified in the second assay. Four previously unknown inhibitors (**64–67**) were identified from this study, Fig. 10. Two of these small molecule inhibitors (**64**, **65**) have a 4-halopyridine scaffold that function as covalent quiescent affinity labels and two are benzimidazole-like inhibitors that reversibly and competitively inhibit human DDAH1. Ebsele was also identified as a potent *hDDAH1* inhibitor from this study, however, this compound binds to multiple targets^{37–39} therefore complicating its use in the clinical setting. A high number of false positives noted in this study highlights the potential challenges in screening new DDAH1 inhibitors.

Current challenges in the development of DDAH1 inhibitors

Since its first discovery of DDAH1 inhibitors about three decades ago there has been slow progress in the development of effective inhibitors. For instance, (i) the current DDAH1 inhibitors have low potency in the micromolar (μM) range; (ii) only a few inhibitors are selective for DDAH1; (iii) almost all DDAH1 inhibitors are based on the arginine scaffold; (iv) the pharmacokinetic characteristics of existing inhibitors have not been thoroughly tested and (v) not a single DDAH1 inhibitor has progressed to human trials.⁹ The main reason for this is that compounds other than arginine/ornithine have not been researched thoroughly for DDAH1 inhibition. It is evident from a comparison of pharmacophore features and the chemical backbone of existing potent *hDDAH1* inhibitors **13**, **20**, **26**, and **60** (Fig. 11) that there is a lack of chemical diversity among these compounds.

DDAH1 inhibitors that mimic the natural substrate (ADMA) are attractive because they are expected to bind to the active site and transported throughout the mammalian body, similarly to

ADMA. Moreover, majority of the arginine based analogues are relatively easy to synthesise with decent yields. However, major limitations of known DDAH1 inhibitors displaying non-specific interactions with NOS and arginase.^{26,28,32} Also for most of the DDAH1 inhibitors (both arginine and non-arginine-like) limited information of their pharmacokinetic profiles are available with only a few studies performed in animal models. Pharmacokinetic data is available for L-257 (**13**), ZST316 (**20**) and ZST152 (**24**)^{40,41} and animal studies detailing the effects of DDAH1 inhibition of L-257 (ref. 34) and DD1E5.¹³

Previously, Rossiter *et al.*¹⁸ tested the selectivity of **13** and **14** (L-257 and L-291 respectively, Fig. 2) towards DDAH1 over other NOS isoforms and were found to be selective for DDAH1. **14** was further characterised for the inhibition of DDAH *in vivo*.³⁴ After administering the inhibitor in mice, plasma ADMA concentrations increased to concentrations that are commonly observed in patients with multiple cardiovascular risk factors.

A recent study conducted by our research group⁴¹ assessed the pharmacokinetics of **20** and **24** (ZST316 and ZST152 respectively, Fig. 3), inhibitors of *hDDAH1*. Intravenous administration of **20** (1.63 h, 60 mg kg⁻¹) displayed a slightly longer half-life compared to **24** (0.86 h at 60 mg kg⁻¹) in mice. However, oral bioavailability was greatest for the lipophilic moiety (**24**, $F = 33.3\%$) than sulfonamide analogue (**20**, $F = 4.7\%$). Sulfonamides are commonly hydrolysed by hepatic carboxylesterase but they may be useful as a prodrug.⁴² Intraperitoneal administration further assessed the pharmacokinetic parameters of **20**. Improved characteristics were observed at 30 mg kg⁻¹ dosage with a half-life of 8 and 6 h, bioavailability of 59–67% and urinary excretion of 54–56% by chronic and acute treatment, respectively. Bioavailability of **20** indicates >50% absorption and excretion concentrations, suggesting the drug is not over metabolised. However, further studies are required to determine whether these compounds display enough drug-like properties for use in humans.

Enzyme inhibitors are often designed with a single target in mind to minimise off-target effects. However, no definitive conclusions have been available on whether dual DDAH1/NOS inhibition could significantly reduce NO concentrations (by direct and indirect NOS inhibition *via* methylarginine accumulation) without showing any negative effects of toxicity in healthy cells. For instance, it is unclear whether such dual inhibition will produce adverse effects by increasing cell toxicity by disrupting NO homeostatic levels required for normal cellular function. Alternatively, dual DDAH1/arginase inhibition is expected to inhibit NO production and simultaneously inhibit the formation of L-ornithine, the product of arginase metabolism necessary for cell proliferation/repair. This is expected to increase endogenous L-arginine concentrations, enabling NO production (*via* NOS) in non-targeted cells thus reducing cell toxicity. Therefore, dual DDAH1/arginase inhibition is proposed as be a useful strategy for selectively targeting tumor growth in multiple cancer phenotypes^{11,43–45} whilst maintaining NO homeostasis in healthy cells. More work assessing *in vivo* effects/benefits of dual DDAH1/arginase and DDAH1/NOS inhibition is needed as knowledge in this area is currently lacking.

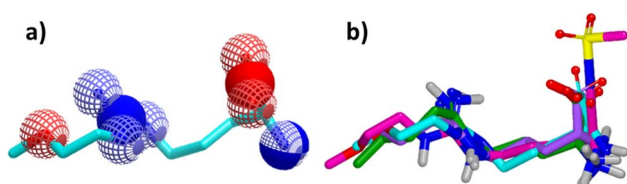


Fig. 11 (a) Hydrogen bond acceptor (red) and donor (blue) atoms of L-257 (**13**). (b) Overlay of *hDDAH1* inhibitors **13** (L-257, cyan), **20** (ZST316, magenta), **26** (purple) and **60** (green). H, N, O and S atoms are shown in white, blue, red and yellow respectively. Images created using OpenEye vROCS⁵⁰ and VIDA.⁵¹



Conclusions and future work

Current DDAH1 inhibitors display only limited structural diversity. Most of the reported reversible hDDAH1 inhibitors are based on ornithine and arginine scaffolds with finite structure activity relationship (SAR) studies.^{18,22,23,26,28,32} None of these compounds inhibit DDAH1 effectively at nanomolar or picomolar concentrations. Moreover, the irreversible inhibitors have not been thoroughly investigated in human DDAH1 isoform. The only inhibitors that selectively inhibit DDAH1 and have minimal effects on arginase and nitric oxide synthase are **13** and **46**. As of now, these inhibitors have not been studied in terms of metabolism and toxicity. The use of structure-based approach to discover and design DDAH1 inhibitors has been limited. More structure guided approaches utilising X-ray crystal structures and rational techniques based on *in silico* design may be needed for the discovery of structurally diverse DDAH1 inhibitors with optimal metabolic profile.

Conflicts of interest

There are no conflicts to declare.

References

- P. Picón-Pagès, J. Garcia-Buendia and F. J. Muñoz, *Biochim. Biophys. Acta, Mol. Basis Dis.*, 2019, **1865**, 1949–1967.
- K. Chen, R. N. Pittman and A. S. Popel, *Antioxid. Redox Signaling*, 2008, **10**, 1185–1198.
- C. Bogdan, *Nat. Immunol.*, 2001, **2**, 907–916.
- K. J. Smith and H. Lassmann, *Lancet Neurol.*, 2002, **1**, 232–241.
- M. S. Winkler, S. Kluge, M. Holzmann, E. Moritz, L. Robbe, A. Bauer, C. Zahrt, M. Priefer, E. Schwedhelm, R. H. Böger, A. E. Goetz, A. Nierhaus and C. Zoellner, *Crit. Care*, 2017, **21**, 189.
- M. C. Martins-Pinge, L. de Jager, B. H. de Campos, L. O. Bezerra, P. G. Turini and P. Pingue-Filho, *Front. Pharmacol.*, 2022, **13**, 1–13.
- C. H. Tengan and C. T. Moraes, *Biochim. Biophys. Acta, Bioenerg.*, 2017, **1858**, 573–581.
- K. M. Miranda, L. A. Ridnour, C. L. McGinity, D. Bhattacharyya and D. A. Wink, *Inorg. Chem.*, 2021, **60**, 15941–15947.
- A. J. Doman, S. Tommasi, M. V. Perkins, R. A. McKinnon, A. A. Mangoni and P. C. Nair, *Bioorg. Med. Chem.*, 2022, **72**, 1–23.
- Z. Wang, S. Lambden, V. Taylor, E. Sujkovic, M. Nandi, J. Tomlinson, A. Dyson, N. McDonald, S. Caddick, M. Singer and J. Leiper, *Biochem. J.*, 2014, **460**, 309–316.
- J.-A. Hulin, S. Tommasi, D. Elliot and A. A. Mangoni, *Biomed. Pharmacother.*, 2019, **111**, 602–612.
- Y. Wang, S. Hu, A. M. Gabisi, J. A. V. Er, A. Pope, G. Burstein, C. L. Schardon, A. J. Cardounel, S. Ekmekcioglu and W. Fast, *ChemMedChem*, 2014, **9**, 792–797.
- K. R. Kami Reddy, C. Dasari, S. Vandavasi, S. Natani, B. Supriya, S. S. Jadav, N. Sai Ram, J. M. Kumar and R. Ummanni, *ACS Comb. Sci.*, 2019, **21**, 241–256.
- J. Leiper, J. Maria, A. Chubb, R. Macallister, I. Charles, G. Whitley and P. Vallance, *Biochem. J.*, 1999, **343**, 209–214.
- V. N. Ragavan, P. C. Nair, N. Jarzebska, R. S. Angom, L. Ruta, E. Bianconi, S. Grottelli, N. D. Tararova, D. Ryazanskiy, S. R. Lentz, S. Tommasi, J. Martens-Lobenhoffer, T. Suzuki-Yamamoto, M. Kimoto, E. Rubets, S. Chau, Y. Chen, X. Hu, N. Bernhardt, P. M. Spieth, N. Weiss, S. R. Bornstein, D. Mukhopadhyay, S. M. Bode-Böger, R. Maas, Y. Wang, A. Macchiarulo, A. A. Mangoni, B. Cellini and R. N. Rodionov, *Nat. Commun.*, 2023, **14**, 3392.
- R. J. Macallister, H. Parry, M. Kimoto, T. Ogawa, R. J. Russell, H. Hodson, G. S. J. Whitley and P. Vallance, *Br. J. Pharmacol.*, 1996, **119**, 1533–1540.
- S. Ueda, S. Kato, H. Matsuoka, M. Kimoto, S. Okuda, M. Morimatsu and T. Imaizumi, *Circ. Res.*, 2003, **92**, 226–233.
- S. Rossiter, C. L. Smith, M. Malaki, M. Nandi, H. Gill, J. M. Leiper, P. Vallance and D. L. Selwood, *J. Med. Chem.*, 2005, **48**, 4670–4678.
- A. J. Hobbs, A. Higgs and S. Moncada, *Annu. Rev. Pharmacol. Toxicol.*, 1999, **39**, 191–220.
- N. M. Olken and M. A. Marletta, *J. Med. Chem.*, 1992, **35**, 1137–1144.
- D. Wang, L. Zou, Q. Jin, J. Hou, G. Ge and L. Yang, *Acta Pharm. Sin. B*, 2018, **8**, 699–712.
- S. Tommasi, C. Zanato, B. C. Lewis, P. C. Nair, S. Dall'Angelo, M. Zanda and A. A. Mangoni, *Org. Biomol. Chem.*, 2015, **13**, 11315–11330.
- J. Kotthaus, D. Schade, J. Kotthaus and B. Clement, *J. Enzyme Inhib. Med. Chem.*, 2012, **27**, 24–28.
- B. R. Babu and O. W. Griffith, *J. Biol. Chem.*, 1998, **273**, 8882–8889.
- L. E. Bretscher, H. Li, T. L. Poulos and O. W. Griffith, *J. Inorg. Biochem.*, 2003, **278**, 46789–46797.
- J. Kotthaus, D. Schade, N. Muschick, E. Beitz and B. Clement, *Bioorg. Med. Chem.*, 2008, **16**, 10205–10209.
- H. Li and T. L. Poulos, *J. Inorg. Biochem.*, 2005, **99**, 293–305.
- I. Lunk, F. A. Litty, S. Hennig, I. R. Vetter, J. Kotthaus, K. S. Altmann, G. Ott, A. Havemeyer, C. Garcia, B. Clement and D. Schade, *J. Med. Chem.*, 2020, **63**, 425–432.
- M. Lluís, Y. Wang, A. F. Monzingo, W. Fast and J. D. Robertus, *ChemMedChem*, 2011, **6**, 81–88.
- J. Murray-Rust, J. Leiper, M. McAlister, J. Phelan, S. Tilley, J. Santa Maria, P. Vallance and N. McDonald, *Nat. Struct. Biol.*, 2001, **8**, 679–683.
- G. Ott, A. Havemeyer and B. Clement, *J. Biol. Inorg. Chem.*, 2015, **20**, 265–275.
- Y. Wang, A. F. Monzingo, S. Hu, T. H. Schaller, J. D. Robertus and W. Fast, *Biochemistry*, 2009, **48**, 8624–8635.
- D. Frey, O. Braun, C. Briand, M. Vašák and M. G. Grütter, *Structure*, 2006, **14**, 901–911.
- J. Leiper, M. Nandi, B. Torondel, J. Murray-Rust, M. Malaki, B. O'Hara, S. Rossiter, S. Anthony, M. Madhani, D. Selwood, C. Smith, B. Wojciak-Stothard, A. Rudiger, R. Stidwill, N. Q. McDonald and P. Vallance, *Nat. Med.*, 2007, **13**, 198–203.



- 35 T. W. Linsky and W. Fast, *Bioorg. Med. Chem.*, 2012, **20**, 5550–5558.
- 36 B. Hartzoulakis, S. Rossiter, H. Gill, B. O'hara, E. Steinke, P. J. Gane, R. Hurtado-Guerrero, J. M. Leiper, P. Vallance, J. M. Rust and D. L. Selwood, *Bioorg. Med. Chem. Lett.*, 2007, **17**, 3953–3956.
- 37 J. Chiou, S. Wan, K.-F. Chan, P.-K. So, D. He, E. W.-C. Chan, T.-H. Chan, K.-Y. Wong, J. Tao and S. Chen, *Chem. Commun.*, 2015, **51**, 9543–9546.
- 38 E. Weglarz-Tomczak, J. M. Tomczak, M. Talma, M. Burda-Grabowska, M. Giurg and S. Brul, *Sci. Rep.*, 2021, **11**, 3640.
- 39 K. Macegoniuk, W. Tabor, L. Mazzei, M. Cianci, M. Giurg, K. Olech, M. Burda-Grabowska, R. Kaleta, A. Grabowiecka, A. Mucha, S. Ciurli and Ł. Berlicki, *J. Med. Chem.*, 2023, **66**, 2054–2063.
- 40 T. Ceruti, R. Frapolli, C. Ghilardi, A. Decio, G. Dellavedova, S. Tommasi, M. Zucchetti and A. A. Mangoni, *Molecules*, 2023, **28**, 8056.
- 41 A. A. Mangoni, T. Ceruti, R. Frapolli, M. Russo, S. Fichera, M. Zucchetti and S. Tommasi, *Molecules*, 2022, **27**, 1017.
- 42 Y. Adriaenssens, D. Jiménez Fernández, L. Vande Walle, F. Elvas, J. Joossens, A. Lambeir, K. Augustyns, M. Lamkanfi and P. Van der Veken, *Org. Biomol. Chem.*, 2017, **15**, 7456–7473.
- 43 X. Wang, H. Xiang, Y. Toyoshima, W. Shen, S. Shichi, H. Nakamoto, S. Kimura, K. Sugiyama, S. Homma, Y. Miyagi, A. Taketomi and H. Kitamura, *Cancer Metab.*, 2023, **11**(1), 1–14.
- 44 J. J. Miret, P. Kirschmeier, S. Koyama, M. Zhu, Y. Y. Li, Y. Naito, M. Wu, V. S. Malladi, W. Huang, W. Walker, S. Palakurthi, G. Dranoff, P. S. Hammerman, C. V. Pecot, K.-K. Wong and E. A. Akbay, *J. Immunotherap. Cancer*, 2019, **7**(32), 1–12.
- 45 J.-A. Hulin, E. A. Gubareva, N. Jarzebska, R. N. Rodionov, A. A. Mangoni and S. Tommasi, *Front. Oncol.*, 2020, **9**, 1–20.
- 46 S. P. Forbes, L. J. Druhan, J. E. Guzman, N. Parinandi, Z. Liwen, K. B. Green-Church and A. J. Cardounel, *Biochemistry*, 2008, **47**, 1819–1826.
- 47 T. Linsky, Y. Wang and W. Fast, *ACS Med. Chem. Lett.*, 2011, **2**, 592–596.
- 48 T. Y. Ghebremariam, C. P. Lependu, A. J. Lee, H. D. Erlanson, P. A. Slaviero, P. N. Shah, P. J. Leiper and P. J. Cooke, *Circulation*, 2013, **128**, 845–853.
- 49 Y. T. Ghebremariam, D. A. Erlanson and J. P. Cooke, *J. Pharmacol. Exp. Ther.*, 2014, **348**, 69–76.
- 50 ROCS 3.6.1.3. OpenEye, *Cadence Molecular Sciences*, Santa Fe, NM, 0, <http://www.eyesopen.com>.
- 51 VIDA 5.0.5.3. OpenEye, *Cadence Molecular Sciences*, Santa Fe, NM, 0, <http://www.eyesopen.comVIDA>.

